Chemical Modification of Wheat Protein-Based Natural Polymers: Grafting and Cross-Linking Reactions with Poly(ethylene oxide) Diglycidyl Ether and Ethyl Diamine

Lusiana Kurniawan,[†] Greg G. Qiao,*[,†] and Xiaoqing Zhang*[,‡]

Polymer Science Group, Department of Chemical and Biomolecular Engineering, The University of Melbourne, Victoria 3010, Australia, and CSIRO Manufacturing & Materials Technology, Private Bag 33, Clayton South MDC, Clayton South, VIC 3169, Australia

Received April 3, 2007; Revised Manuscript Received June 12, 2007

Mobile poly(ethylene oxide) diglycidyl ether (PEODGE) segments were chemically grafted onto a soluble wheat protein (WP), and different network structures were formed via coupling reactions with ethyl diamine (EDA) in different PEODGE/EDA (PE) ratios. When the PE ratio was 1:1, linear PEs were the predominant segments grafted onto WP chains and the whole WP−PEODGE−EDA (WPE) system was still soluble with an increased molecular weight. Reducing the amount of EDA in the systems produced insoluble cross-linked WPE networks. The broad distribution of network structures and chain mobility resulted in a broad glass transition for the WPE materials. However, the glass transition started at lower temperatures, and the materials became flexible at room temperature. The PE segments were present in all rigid, intermediate, and mobile phases in WPE networks, while the proportion of mobile WP chains was increased as a result of the plasticization effect from the mobile PE segments. The mobility of the most mobile component lipid was also restricted to some extent when forming the cross-linked WPE networks. The study demonstrated that the formation of different network structures with PE segments could significantly improve the flexibility of WP materials, vary the solubility, and modify the mechanical performance of WP-based natural polymer materials.

1. Introduction

Wheat proteins (WPs), as one of the most interesting plant proteins, have demonstrated a series of polymer properties such as strong tensile strength, good viscoelastic properties, and excellent gas barrier performance when used in packaging, coating, and medical applications.[1−10] There are strong interactions within WP involving intermolecular and intramolecular associations in conjunction with cross-linking via disulfide bonds. Consequently, WP films are usually brittle and difficult to meet many application requirements. Normally a large amount of plasticizer is used in producing WP films via either solution casting or thermal processing.[11−18] These plasticized materials have difficulty in retaining their properties in packaging or medical applications after exposure to wet conditions because the plasticizers, usually water, glycerol, polyols, or amines, can be extracted from the materials. It has been a challenging task for polymer material scientists to chemically modify the molecular structure of WPs in order to enhance the flexibility of the WP macromolecules and their processing capability, thus extending the applications of the natural polymer.

The chemical modification of proteins through chemical reactions between amino groups of proteins and compounds containing epoxy groups has been reported previously for biomedical applications.[19,20] Poly(ethylene oxide) diglycidyl ether (PEODGE) is an interesting polymer segment with two reactive epoxy end groups in each chain that can react with the amino groups of gelatin under mild conditions.[19−21] In this work, the objective was to obtain a cross-linked WP−polymer network via grafting PEODGE onto the protein macromolecules via reactions between the epoxy groups in PEODGE and the amino groups of WP, and then coupling the excess PEODGE with the grafted PEODGE segments by the addition of ethylene diamine (EDA), a compound containing two primary amine groups (Scheme 1). Each PEODGE chain has two glycidoxy end groups, while EDA has two $-NH_2$ groups. Because the amount of amino groups in WP is very low (mainly on the side chains of lysine), and only a small proportion of PEODGE can graft onto WP, the initial addition of an excess amount of PEODGE prior to the addition of EDA will ensure the grafting of PEODGE to WP. Because of a small amount of these amino groups in WP, the PEODGE/EDA (PE) ratio determines the structure of the WP−PEODGE−EDA (WPE) networks, similar to the case when only PEODGE and EDA were used.[22] When the mole ratio of PE was 1:1, linear PE segments were formed predominantly with a structure of $-(NH-CH_2-CH_2-NH-CH_2-CHOH-CH_2-O-PEO-CH_2-CHOH-CH_2)_n-$ as branched chains to the WP. Reducing the amount of EDA should lead to some proportion of the >NH groups on the PE segments further reacting with the extra PEODGE and forming cross-linked structures within the WPE matrix.[22] Additional epoxy groups could also remain in the matrix when the amount of EDA is not sufficient for the reactions. Modifying these WP materials by varying the ratio of PEODGE to EDA would provide the possibility for further chemical reactions by introducing new functional groups such as >NH, −OH, and epoxy groups to the materials.

The grafting and coupling reactions between WP and PE were studied by high-resolution nuclear magnetic resonance (NMR) spectroscopy. The WPE products were further processed into plastic sheets by thermal compression molding. The mechanical

* Corresponding author. Tel: +61383448665. Fax: +61383444153. E-mail: gregghq@unimelb.edu.au. (G.Q.). Tel: +61395452653. Fax: +61395441128. E-mail: Xiaoqing.Zhang@csiro.au. (X.Z.).

[†] The University of Melbourne.

[‡] CSIRO Manufacturing & Materials Technology.

10.1021/bm0703719 CCC: $37.00
Published on Web 07/31/2007

Scheme 1. Grafting PEODGE onto WPs and Then Forming a WPE Cross-Linked Network

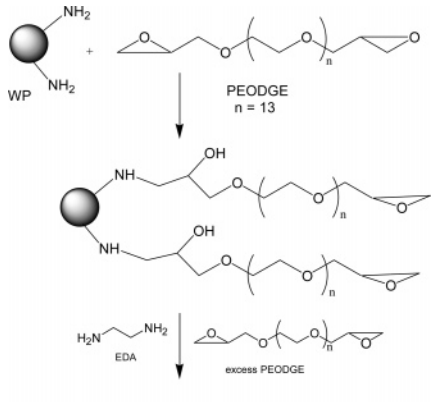

WP-PEODGE-EDA Cross-linked Network

properties, glass transition temperatures, and molecular motions of these systems were examined by dynamic mechanical analysis (DMA) and broad-line solid-state NMR techniques. The use of high-resolution solid-state NMR to study the molecular motions of each individual component in the complicated network and the phase structures of the whole network achieved a good understanding between the mechanical performance of the materials and their macromolecular motions/phase structures.

2. Experimental Section

2.1. Materials. A deamidated soluble WP, which contained over 90% protein, 5% lipid, and a small amount of residual starch with other minor impurities, was used in this work, as supplied by Manildra Group Australia. The deamidation was conducted under mild conditions, resulting in 30−35% of amides (−$CONH_2$) in the side chains being broken, resulting in −COOH as the end groups. The natural moisture content of the WP was 7−8%. PEODGE (M_w = 730) was purchased from Polyscience, Inc., while EDA (>99.5%) was obtained from Aldrich Fine Chemicals (Australia). Distilled water was used as the solvent in all experiments, and all reactions were conducted at room temperature.

2.2. Sample Preparation. PEODGE and WP were mixed in water using a high sheer mixer operated at 4000 rpm for 2 h in order to achieve an efficient reaction between the amino groups in WP and the epoxy groups of PEODGE. EDA was then added to the system, and additional reactions were conducted under mechanical stirring at 400 rpm for 72 h. The PE polymer component was kept at 20 wt % in WP−PE systems, but the mole ratio of PEODGE to EDA was varied as 1:1 (WPE11), 2:1 (WPE21), and 3:1 (WPE31). After reactions, the obtained solutions were dried overnight under ambient temperature, and then further dried in a vacuum oven at 40 °C for 3 days. The moisture content in the samples was 8−9%, as determined by thermogravimetric analysis (TGA). Compression molding was conducted under an optimum condition of 130 °C for 5 min using a heating press with a pressure of 12 ton. The pressing area was 145 mm × 145 mm, and the thickness of the samples was 1.0 mm ± 0.1 mm. The final moisture content of the compression-molded plastic sheet samples was 5−6%, as measured by TGA.

2.3. Sample Characterization. The molecular weights of WP and the soluble components in WPE samples were measured by gel permeation chromatography (GPC). A triple detection system including a Wyatt Dawn F laser photometer operating at 90° (right angle laser light scattering) coupled with an online Waters 410 differential refractometer (for measurement of the refractive index) and a Viscotek T50A differential viscometer (for measurement of the differential pressure) was used. The three detectors were calibrated with Pullulan standards of known molecular weight and intrinsic viscosity and narrow polydispersity. A Shodex P-82 column from Phenomenex was used, and data acquisition and analysis were performed with Viscotek TriSEC software. Solutions of WPE materials with a concentration of 20 mg/mL were prepared by redissolving the samples in an appropriate amount of water. GPC experiments were conducted with water as the mobile phase under a flow rate of 1.0 mL/min. The injection volume was 20 μL, and the column temperature was 30 °C.

Table 1. Molecular Weight of the Soluble Components in WP, WPE11, WPE21, and WPE31 as Measured by GPC

sample	solubility	M_n	M_w
WP before shearing	100%	200 600	236 500
WP after 2 h shearing at 4000 rpm	100%	71 500	89 800
WPE11	95%	135 400	142 300
WPE21	7%	114 800	153 700
WPE31	1−2%		

DMA experiments were operated on a Perkin-Elmer PYRYS Diamond DMA in dual cantilever bending mode at a frequency of 1 Hz. The temperature was set at −100 to 160 °C, and the heating rate was 2 °C/min. The storage modulus (E'), loss modulus (E'') and tan δ (E'/E'') were recorded as a function of temperature throughout the experiment. The value of E' is calculated as the ratio of the stress to the applied strain as a measure of the stiffness or rigidity of the material, while E'' reflects the ability of a material to dissipate mechanical energy by converting it to heat through molecular motions. The term tan δ is a useful index of material viscoelasticity.[23,24]

Broad-line pulse ^{1}H NMR was carried out on a Bruker Minispec PC 120 spectrometer at 20 MHz at 40 °C. The 90° pulse was 4.5 μs with a repetition of 2 s. The free induction decay (FID) signal of each sample was obtained by a solid-echo pulse sequence[25] and a Carr−Purcell−Meiboom−Gill (CPMG; $90°x - (\tau_1 - 180°y - \tau_1 - \text{echo})_n$) pulse sequence,[25] respectively. The 90°−90° pulse spacing in the solid-echo was 10 μs, and the dwell time was 1.25 μs. The 90°−180° pulse spacing (τ_1) in the CPMG sequence was 50 μs, n was varied, and a total of eight scans were used for each measurement. The whole FID of each sample was a combination of the data observed from solid-echo (time range of 0−0.2 ms) and from CPMG (time range of 0.2−10 ms) pulse sequences, and then a multidecay function was used to best fit the FID data with the IGOR program from Wave Metrics, Inc., as described in previous papers.[18,26]

High-resolution solid-state NMR experiments were conducted at room temperature using a Varian Unity plus spectrometer at resonance frequencies of 75 MHz for ^{13}C and 300 MHz for ^{1}H. ^{13}C NMR spectra were observed either under cross-polarization (CP), magic-angle spinning (MAS), and high-power dipolar decoupling (DD) technique, or using a single 90° pulse excitation (SPE) method with high-power decoupling. The 90° pulse was 4.5 μs for ^{1}H and ^{13}C, the radio frequency strength for spin-locking was 56 kHz, while the spinning rate of MAS was around 7 kHz. A contact time of 1.0 ms was used for measuring the CP/MAS spectra, while the repetition time was 2 s for all measurements. The chemical shift of ^{13}C spectra was determined by taking the carbonyl carbon of solid glycine (176.03 ppm) as an external reference standard. ^{1}H MAS NMR spectra were obtained with the same MAS rates, and tetramethylsilane was used as an external chemical shift reference.

^{1}H spin−spin (T_2) relaxation times under high-resolution conditions (MAS) were measured through the decay of ^{1}H intensities in the MAS spectra observed by the CPMG pulse sequence[25] (τ_1 of 40 μs), with a repetition time of 2 s and a 90° pulse length of 2.5 μs. The ^{1}H T_2 data were also measured through the change of ^{13}C magnetization prepared by CP with varied CP delay times, as reported previously.[18,27−29]

3. Results and Discussion

3.1 Grafting and Coupling Reactions between WP and PE. The use of a water-soluble WP via deamidation has made it possible to expose most of the amino groups in the WP

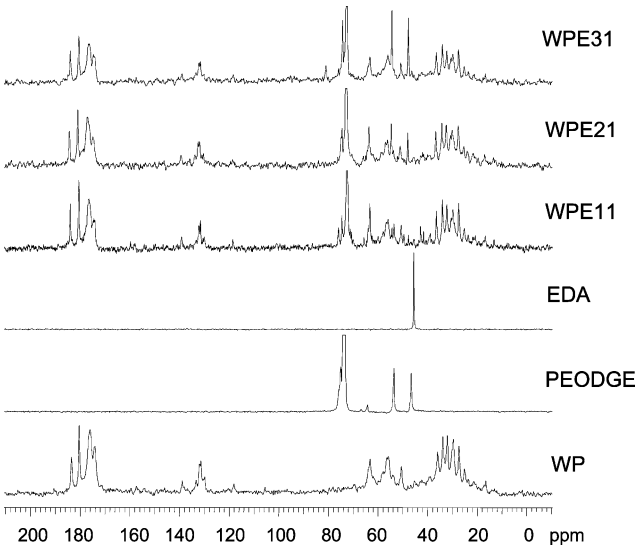

Figure 1. ^{13}C solution NMR spectra of WP, PEODGE, EDA, WPE11, WPE21, and WPE31 systems after reaction in water solution.

macromolecules to take part in grafting reactions with the epoxy groups of PEODGE in water media. In order to achieve homogeneous mixing and complete reactions of grafting and the following coupling reaction, each WP/PEODGE solution was mixed under high shearing conditions (4000 rpm) for 2 h, and the coupling reactions with EDA were conducted for 3 days under slow stirring. The solubility of the systems and the molecular weight of the soluble proportion in the systems changed significantly after grafting−coupling reactions when using varied ratios of PEODGE to EDA, as shown in Table 1. The soluble WP had a molecular weight of 236 500 (M_w). Mixing under high shearing caused a reduction in the molecular weight to 89 800 (M_w); however, this is not an issue if a highly cross-linked network is eventually formed. When PEODGE and subsequent EDA were introduced into the WP systems at a PE ratio of 1:1 (WPE11), the majority of components in the system were still soluble (solubility of 95%); however, the molecular weight of the soluble proportion increased to 142 300 (M_w) as the result of grafting and coupling reactions. The high solubility of the system was attributed to the formation of linear PE segments as the predominant products at this PE ratio. When the PE ratio was increased, the solubility decreased significantly: down to 7% when PE = 2:1 (WPE21), and only 1−2% when PE = 3:1 (WPE31), indicating the formation of highly cross-linked structures in the WPE21 and WPE31 systems.

^{13}C solution NMR spectra of WP, PEODGE, EDA, and the soluble components in the WPE systems are shown in Figure 1. The spectrum of WP was similar to those obtained previously with the reported assignment. The strong intensity at 72.8 ppm of PEODGE was due to the ethylene resonances of the PEO segment, while two sharp peaks at 52.9 and 45.8 ppm (>CH and $>CH_2$) were attributed to the epoxy end groups. The ethylene resonance of EDA was observed at 45.4 ppm. After WP reacted with PEODGE and EDA under the described conditions, for WPE11, the sharp peak of EDA and the glycidoxy resonances all disappeared, while some new resonances appeared at 75.3, ~54, and ~42 ppm, corresponding to the species of −CHOH, −CHNH−, and $-CHNH_2$ formed in the reactions. When the amount of EDA was reduced (WPE21 and WPE31), unreacted glycidoxy structures or excess PEODGE could be observed in the NMR spectra of the soluble part in the systems, but it should be remembered that the solubility was only 7% or 1−2% for WPE21 and WPE31, respectively.

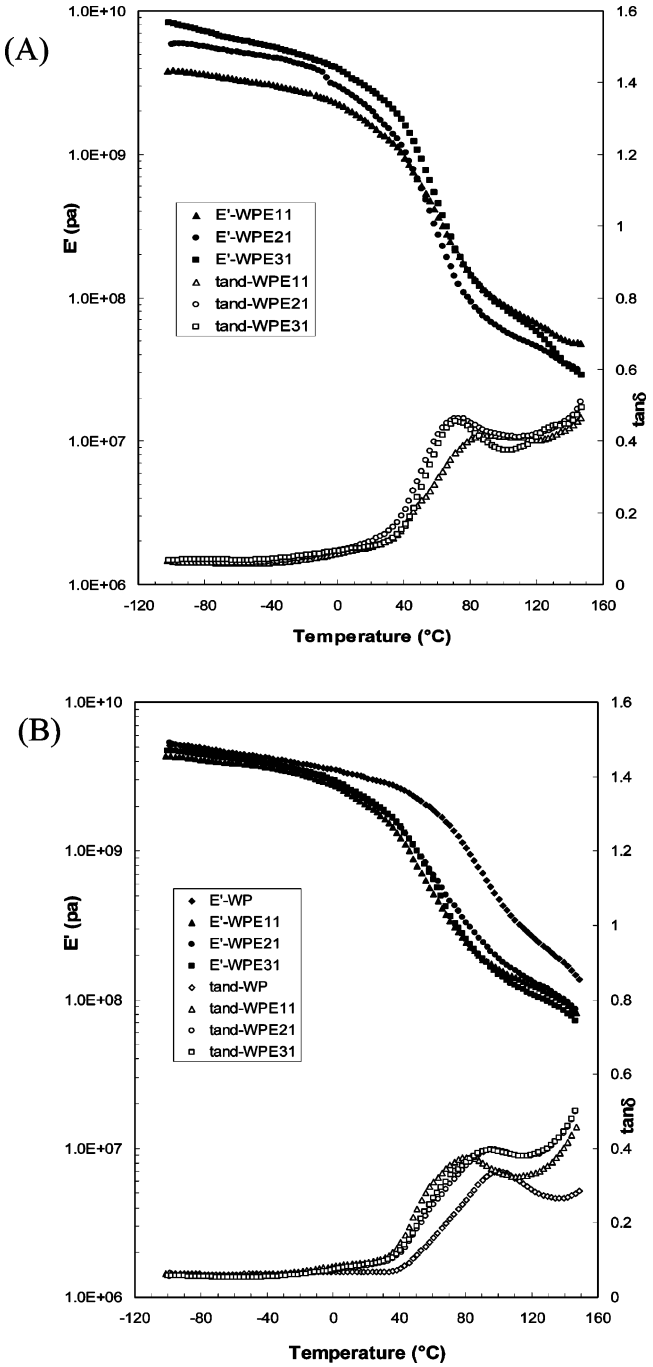

Figure 2. Storage modulus (E') and tan δ of WP, WPE11, WPE21, and WPE31 samples as obtained via DMA: (A) solution-cast samples and (B) compression-molded samples.

The results indicate that the grafting and coupling reactions produced WPE networks with different structures as a result of the different ratios of PE.

3.2 Mechanical Properties of the WPE Materials. The WPE materials obtained via solution casting were further thermally processed by compression molding into plastic sheet samples. The DMA results of these solution-cast and thermally processed samples are shown in Figure 2. The general trends of DMA data for the WPE systems were similar to those of plasticized WP-based materials.[16−18,26] For solution-cast samples, the E' of WPE11 at a low temperature range (far below the glass transition temperature T_g) was relatively lower. It increased for WPE21, with even higher E' values for WPE31 at the same temperature range. The tan δ peaks corresponding to the T_g

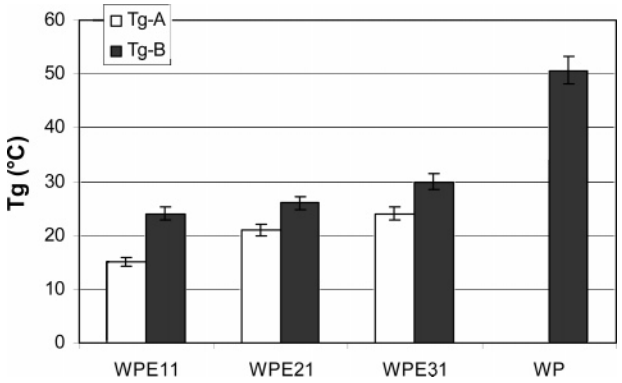

Figure 3. The $T_{g-start}$ data obtained from the onset of storage modulus E' decrease (corresponding to T_g transition) of WPE11, WPE21, WPE31, and WP. Tg-A: solution-cast samples; Tg-B: compression-molded samples.

transitions of the WPE systems were all very broad, especially for WPE11, while those of WPE21 and WPE31 were quite similar. It appeared that the distribution of grafting structures was broad, and cross-linking caused an effect on motional homogeneity. In addition, the maximum value of tan δ was higher for WPE21 and WPE31 as compared to that of WPE11, suggesting a more pronounced effect on the mobility of the whole materials from the mobile segments of PE. The solution-cast sample of WP (especially after shearing at 4000 rpm for 2 h) was too brittle to handle for conducting a DMA test. Thermal compression molding of WPE11, WPE21, and WPE31 seemed to average out the differences among the three WPE systems, resulting in similar E' behaviors of the systems as the temperature increased. However, the T_g of the WPE materials was significantly reduced compared to that of WP, as the tan δ peaks corresponding to the T_g transitions for the WPE systems were all shifted to lower temperatures (Figure 2B). The β-transition of the WP materials (around -60 °C) was not found in the E' and tan δ curves for all materials, possibly because of the low moisture content in the systems (8−9% in solution-cast samples and 5−6% in compression-molded samples).

The temperatures when the glass transition started ($T_{g-start}$) for these WPE plastics were measured by taking the onset of the E' decrease corresponding to the T_g transition and are plotted in Figure 3. Because of the mobile nature of PE segments, the WPE systems always showed a lower $T_{g-start}$ value at around 15−30 °C as compared to that of the WP sample (51 °C) with a similar moisture content, indicating that the WPE materials became more flexible at room temperature. Note that the $T_{g-start}$ values of WPE systems also relied on the ratio of PE and the processing conditions when the same 20 wt % of PE was used in all WPE systems. The formation of linear PE segments attached to a WP matrix resulted in the lowest T_g value, while high T_g values were obtained when WPE21 and WPE31 systems formed cross-linked network structures for both solution-cast and compression-molded samples. The tan δ peaks (corresponding to T_g) reached maximum intensities at around 70−80 °C (or 80−95 °C) for WPE solution-cast (or thermally processed) samples. Thermal processing produced an additional effect in the systems, and thus gave rise to a further increase in the T_g values for the materials.

A previous study[22] of PEODGE and EDA systems showed that a PE ratio of 1:1 produced a linear polymer, while a PE ratio of 2:1 gave a cross-linked network structure. However, further increase of PE ratio to 1:3 resulted in a branched polymer. If assuming that minimal epoxy groups of PEODGE were involved in grafting reactions with the amino groups of WP, then WPE21 (PE = 2:1) would form the network with the highest cross-linked density, while branched structures were formed in the WPE31 system. However, the highest E' in the low-temperature range and the highest T_g values were actually obtained for WPE31, which is contrary to what is found by simply considering the branching effect on the WP matrix. These results suggest that the epoxy groups of the PE segments in WPE31 could also react with other functional groups of WP and even the hydroxy groups of residual starch in the systems, especially under the thermal processing conditions. These additional chemical linkages formed between the WP matrix and PE segments would act as an additional cross-linking effect to the material performance. The true effect of the cross-linking on the molecular motions of WPE systems is very complicated, this solid-state NMR techniques were then applied to explore the structural and motional information of the WPE systems.

Table 2. ^{1}H T_2 Data of the Compression-Molded WPE Materials from Combined FID via Solid-Echo and CPMG Measurements[a]

samples	T_{2S} (μs)	A_{2S} (%)	T_{2M} (μs)	A_{2M} (%)	T_{2L} (μs)	A_{2L} (%)
WP	9.8	71	110	18	890	11
WPE11	9.6	53	48	33	840	14
WPE21	9.4	54	44	32	760	14
WPE31	9.9	58	87	37	780	5

[a] Error of 5−8%.

3.3. Molecular Motions and Phase Structures of the WPE Network. WP contains a series of different nature components, such as proteins, lipids, and moisture, that could interact or be chemically attached to the PE segments in the WPE network. The different network structures formed by using different PE ratios could also result in different effects on the molecular motions, as seen in the DMA results. The investigation of the molecular motions of each component and the phase structures of the whole network is important for understanding the interactions among different components in such complicated WPE systems. Solid-state NMR techniques have provided powerful tools to examine the molecular motion and phase structure of the WPE networks.

Analysis of the T_2 data provides information on both the motional nature (the T_2 value) and the proportion of each motional component (the intensity of the T_2 component) of a multicomponent/phase polymer system.[25] The ^{1}H T_2 is sensitive to the T_g transition of polymer materials. At a temperature far below T_g, the T_2 of a polymer is usually not sensitive to an increase in temperature because of the static dipolar interaction in the rigid polymer. An FID with a fast Gaussian decay giving a short T_2 time is normally observed, which is independent of temperatures below the T_g. The T_2 increases significantly at the T_g, and above the T_g, the exponential decay is slow, resulting in a long T_2 that is very sensitive to slow frequency motions.

The ^{1}H T_2 data of the compression-molded WPE samples obtained by combination of the FID signals measured via solid-echo and CPMG pulse sequences at 40 °C, a temperature above the $T_{g-start}$ but below the tan δ maximum (corresponding to T_g) of all WPE samples, are listed in Table 2. All of the systems generated three T_2 components (T_{2S}, T_{2M}, and T_{2L}) from the FID analysis, including WP with a $T_{g-start}$ of 51 °C. These three components describe a less plasticized protein phase (T_{2S} phase), a plasticized phase (T_{2M} phase) and a mobile phase (T_{2L} phase) containing plasticizers and lipid.[18] The WP sample displayed a short T_2 component (T_{2S}, 9.8 μs) corresponding to a rigid phase (71%), while the T_{2M} and T_{2L}, with values of 110 and 890 μs, respectively, reflected an intermediate phase (18%) and a mobile phase (11%) in the material. When PE segments were introduced

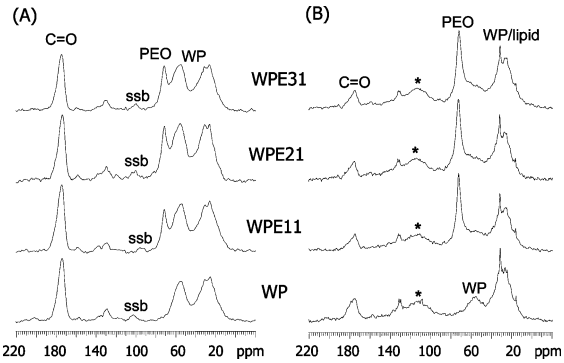

Figure 4. ^{13}C CP/MAS (A) and SPE (B) NMR spectra of the compression-molded WP, WPE11, WPE21, and WPE31 samples.

into the WP matrix, the T_{2S} remained in the range of 9.5 to 9.9 μs, while the T_{2S} proportion (A_{2S}) decreased from 71% to 53−58% because 20% of the mobile PE was introduced into these WPE systems. The minor difference in A_{2S} among these WPE systems is possibly attributed to the formation of different WPE network structures. In WPE11, the linear PE segments grafted onto WP mainly played a plasticizing role on WP, thus reducing the proportion of the rigid phase in the material. When the amount of EDA was reduced, cross-linked structures were formed that caused the polymer segments next to the cross-linked points to become rigid and then contribute to the T_{2S} phase. Note that the highest A_{2S} for WPE systems was obtained in WPE31. A large proportion of PE segments contributed to the intermediate (T_{2M}) phase as the A_{2M} proportion increased to 33−37% from 18% for WP, and remained relatively constant in all WPE systems. The T_2 value of the T_{2M} phase decreased to 44−48 μs for WPE11 and WPE21 as compared to 110 μs for that of WP, but it then increased to 87 μs for WPE31. It seemed that these PE segments were less mobile than that of plasticized WP. The relatively longer T_{2M} in WPE31 could be due to the contribution from other mobile components in WP associated with the cross-linked network; note that the A_{2L} was only 5% for WPE31. The T_{2L} values of WPE were all lower than that of WP, suggesting that moisture and lipids could also associate to the networks to some extent. The wide distribution of mobility in different phases caused a broad tan δ peak corresponding to the T_g transition, as shown in Figure 2.

High-resolution solid-state NMR techniques were applied to detect ^{13}C NMR spectra of the WPE networks. The CP/MAS/DD method is sensitive to the rigid components of materials, as the enhancement of the carbon signals is due to the polarization transfer from protons to nearby carbons via strong dipolar interactions in rigid polymers. On the other hand, the SPE method with a repetition time as short as 2 s is sensitive to the mobile components of a polymer system. The ^{13}C CP/MAS and SPE spectra of WP and WPE materials are shown in Figure 4 with resonance assignment as reported in previous papers.[16−18] Note that the PEO signal of PE segments at 72 ppm[27] were not only detected in the SPE spectra, but also in the CP/MAS spectra, suggesting a wide distribution of the mobility of the PE segments and strong interactions between WP and PE segments due to the chemical linkages and hydrogen bonding interactions via various polar functional groups within the two components.

The resonances of WP and the PEO of PE segments do not overlap each other in the ^{13}C NMR spectra (Figure 4), thus the behaviors of WP and PE components in the networks can be examined individually from the NMR relaxation parameters observed at these resonances. The ^{13}C CP/MAS NMR spectra of a WPE21 sample observed with varied CP delay times are

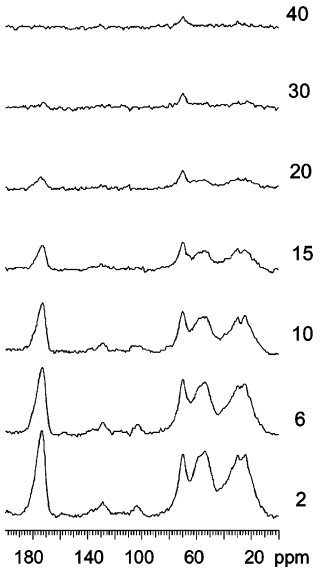

Figure 5. ^{13}C CP/MAS NMR spectra of the compression-molded WPE21 sample measured with varied CP delay times (τ), where the ^{13}C intensity follows ^{1}H T_2 decay.

Table 3. ^{1}H T_2 Values (μs) of the Compression-Molded WPE Materials from ^{13}C CP/MAS Spectra[a]

samples	WP @ 173 ppm	PE @ 72 ppm	WP @ 55 ppm	WP @ 25 ppm
WP	14.7		14.1	15.4
WPE11	13.5	12.3/48%	13.0	13.7
		37.2/52%		
WPE21	13.0	12.2/49%	13.7	13.3
		41.5/51%		
WPE31	13.2	12.8/57%	13.1	14.8
		56.1/43%		

[a] Error of 5−8%.

shown in Figure 5. After the 90° pulse in the proton channel, the intensities of proton resonances decreased with an increase in CP delay time following ^{1}H T_2 decay, and such intensity variation transferred to the ^{13}C resonances observed via CP.[26,27] At a short CP delay time, the observed ^{13}C resonances reflected all WPE21 resonances enhanced via CP. As the CP delay increased, these resonances decreased their intensities following ^{1}H T_2 decays. The WP resonances in all WPE systems displayed a fast Gaussian decay with a single T_2 value, while the intensity at 72 ppm (PE) decayed slower, showing a combination of a fast Gaussian and a slow exponential decay. Certainly, more mobile components such as lipids or free PE (if it existed) would be missed by CP/MAS observation because of their weak CP capability due to fast molecular motions.

The T_2 values of the WP and WPE samples observed by the CP/MAS method are listed in Table 3. The ^{1}H T_2 data of the WP sample observed from all ^{13}C resonances were identical at 14−15 μs. When the mobile PE segments were introduced into the WP system, the observed T_2 values from the WP resonances still remained in a similar range of 13−14 μs, irrespective of the PE ratio. The T_2 values observed from the PE resonance at 72 ppm displayed two-component decays. The values of the short T_2 components were around 12−13 μs in all WPE samples, but the proportion of this component increased slightly as the EDA content decreased. The values of the longer T_2 component observed at 72 ppm were similar to those of T_{2M} shown in Table 2, and the proportion of this component decreased slightly when the EDA content decreased, indicating that some of the PE

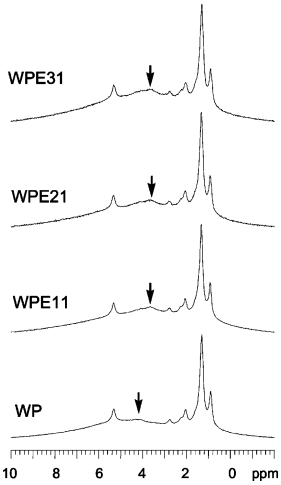

Figure 6. ^{1}H MAS NMR spectra of the compression-molded WP, WPE11, WPE21, and WPE31 samples. The arrow shows the shift of the broad peak from 4.2 ppm in WP to 3.5 ppm in WPE systems.

segments became rigid when forming cross-linked WPE networks. The difference in CP capability among these phases caused the phase composition to not be directly related to the proportions of the T_2 components presented in Table 3. The limited numbers of chemical linkages between WP and PE cannot explain the significant amount of rigid PE component measured, even in WPE11. It is possible that the strong interactions (possibly hydrogen bonding) between PE and WP segments due to the large amount of polar groups in both components may immobilize the PE segments to a great extent. The results indicate that the T_{2S} components in the WPE systems shown in Table 2 should consist of a certain level of PE segments strongly interacting with WP to become rigid, while the T_{2M} components could include an increased contribution from WP chains plasticized by other mobile PE segments. The relatively longer T_{2M} value for WPE31 (Table 2**)** and the longer T_2 value observed at 72 ppm (Table 3) reflect the mobile nature of the PE network when the amount of EDA was lower and free mobile PEODGE chains could remain in the system. Even though the T_{2M} phase in WPE31 was relatively mobile, the lowest proportion of mobile component and the highest amount of rigid phase still produced the highest T_g for the WPE31 system.

The most mobile components in the WPE systems were examined by ^{1}H MAS spectra via the CPMG pulse sequence, as shown in Figure 6. Lipid and water signals detected in WP were similar to those reported previously for plasticized WP systems.[16−18,26] However, the broad peak around 4.2 ppm (moisture) in WP shifted to around 3.5 ppm in the WPE systems, suggesting a contribution from some very mobile PE segments (−C**H**$_2$−C**H**$_2$−O−) to these broad peaks. The ^{1}H T_2 values of the water, PE, and lipids obtained via the CPMG/MAS method are listed in Table 4. Note that the ^{1}H T_2 values observed from the broad peak around 3.5 ppm for WPE networks were quite similar to each other but slightly longer than that observed at 4.2 ppm for WP, suggesting that the PE segments detected by this method were slightly more mobile than the moisture in WP. The moisture remaining in the WPE networks should mainly be the bound water at a moisture content as low as 5−6 wt %,[18] and fast chemical exchange within the system would average out the difference in the mobility of these water molecules associated with different species. The T_2 data observed for WPE systems at 3.5 ppm reflect an average mobility of these very mobile PE segments and the bound water associated with WPE segments via hydrogen bonding interactions. The high-resolution solid-state NMR studies indicated that there was a broad mobility distribution of PE segments in the WPE networks; the PE segments existed in all rigid, intermediate, and mobile phases of the systems.

Table 4. ^{1}H T_2 Values (ms) of the Moisture and Lipid in Compression-Molded WPE Materials via ^{1}H MAS Spectra[a]

samples	moisture and PE @ 4.5−3.5 ppm	lipid @ 5.5 ppm	lipid @ 2.1 ppm	lipid @ 1.3 ppm	lipid @ 0.9 ppm
WP	0.23	0.53	2.9	7.7	5.5
WPE11	0.27	0.60	1.8	7.8	6.4
WPE21	0.28	0.46	1.4	6.7	5.3
WPE31	0.27	0.41	1.0	6.5	4.6

[a] Error of 2−6%.

The lipid in WP is usually associated with protein chains with the assignment of lipid previously reported.[29] The formation of WPE networks restricted the mobility of the lipid, especially when cross-linked structures were formed, as seen in Table 4. Note that each resonance in lipid displayed a different motional restriction effect. The T_2 data of −C**H**$_2$−COO− protons at 2.1 ppm decreased in all WPE samples, indicating that the interactions between the −COO− groups of lipid and the WPE networks (most likely the PE segments) were stronger than those between lipids and WPs. The −C**H**$_2$− on the lipid chains (1.3 ppm) and the −C**H**$_3$ groups (0.9 ppm) are not involved at the interaction centers, thus T_2 only decreased slightly in WPE21 and WPE31 networks. The difference between the ^{1}H T_{2L} values in Table 2 and those of lipid and water in Table 4 is partially due to the difference in measurement methods. The application of MAS effectively averaged the dipolar interactions of the mobile species such as water and lipid, thus their T_2 became much longer under MAS conditions. On the other hand, some proportion of moisture or lipid might contribute to the T_{2M} phase in WPE31, which would be missed by CPMG/MAS observation.

4. Conclusions

The mobile PEODGE segments were chemically grafted onto a soluble WP, and different network structures were formed via coupling reactions with EDA in different ratios. When the PE ratio was 1:1, linear PEs were the predominant segments grafted onto WP chains and caused the molecular weight of WPE11 to increase. Reducing the amount of EDA in the WPE systems resulted in the formation of cross-linked polymer networks and a significant decrease in the solubility of the materials. The WPE systems exhibited a wide structure and mobility distribution, thus resulting in a broad T_g transition for the materials. In general, the WPE materials were flexible at room temperature, and the T_g shifted to lower temperatures compared to that of WP alone. The chemical bonding and strong intra- and intermolecular interactions between the WP and PE segments resulted in a broad distribution of molecular motions of the WPE materials. The PE segments were present in all rigid, intermediate, and mobile phases, while the proportion of mobile WP chains was increased due to the plasticization effect from the mobile PE segments. The mobility of the most mobile component lipid was also restricted to some extent when forming the cross-linked WPE networks. This study demonstrated that the formation of different network structures with PE segments could significantly improve the flexibility of WP materials, vary the solubility, and modify the mechanical performance of WP-based natural polymer materials.

References and Notes

(1) Mangavel, C.; Barbot, J.; Gueguen, J.; Popineau, Y. *J. Agric. Food Chem.* **2003**, *51*, 1447−1452.
(2) Gontard, N.; Guilbert, S.; Cuq, J. L. *J. Food Sci.* **1992**, *57*, 190−195.
(3) Gennadios, A.; Weller, C. L.; Testin, R. F. *Cereal Chem.* **1993**, *70*, 426−429.
(4) Micard, V.; Belamri, R.; Morel, M. H.; Guilbert, S. *J. Agric. Food Chem.* **2000**, *48*, 2948−2953.
(5) Belton, P. *J. Cereal Sci.* **1999**, *29*, 103−107.
(6) Derksen, J. T. P.; Cuperus, F. P.; Kolster, P. *Prog. Org. Coat.* **1996**, *27*, 45−53.
(7) Ornebro, J.; Nylander, T.; Eliasson, A. *J. Cereal Sci.* **2000**, *31*, 195−221.
(8) Singh, H.; Macritchie, F. *J. Cereal Sci.* **2001**, *33*, 231−243.
(9) Scott, G. *Degradable Polymers: Principles and Applications*, 2nd ed.; Kluwer Academic Publishers: Dordrecht, The Netherlands, 2002.
(10) Kester, J. J.; Fennema, O. *Food Technol.* **1986**, *40*, 12−47.
(11) Mangata, J.; Bauduin, G.; Boutevin, B.; Gontard, N. *Eur. Polym. J.* **2001**, *37*, 1533−1541.
(12) Gontard, N.; Guilbert, S.; Cuq, J. L. *J. Food Sci.* **1993**, *58*, 206−211.
(13) Li, M.; Lee, T. *J. Agric. Food Chem.* **1996**, *44*, 1871−1880.
(14) Redl, A.; Morel, M.; Bonicel, J.; Vergnes, B.; Guilbert, S. *Cereal Chem.* **1999**, *76*, 361−370.
(15) Redl, A.; Morel, M.; Bonicel, J.; Vergnes, B.; Guilbert, S. *Rheol. Acta* **1999**, *38*, 311−320.
(16) Zhang, X.; Burgar, I.; Lourbakos, E.; Beh, H. *Polymer* **2004**, *45*, 3305−3312.
(17) Zhang, X.; Burgar, I.; Do, M. D.; Lourbakos, E. *Biomacromolecules* **2005**, *6*, 1661−1671.
(18) Zhang, X.; Do, M. D.; Hoobin, P.; Burgar, I. *Polymer* **2006**, *47*, 5888−5896.
(19) Van Wachem, P. B.; Zeeman, R.; Dijkstra, P. J.; Feijen, J.; Hendriks, M.; Cahalan, P. T.; Van Luyn, M. J. A. *J. Med. Res.* **1999**, *47*, 270−277.
(20) Sung, H. W.; Huang, D. M.; Huang, R. N.; Hsu. J. C. *J. Med. Res.* **1998**, *46*, 520−530.
(21) Lee, H.; Neville, K. *Handbook of Epoxy Resin;* McGraw-Hill, Inc.: New York, 1967; Chapter 5.
(22) Kwok, A.; Qiao, G.; Solomon, D. H. *Chem. Mater.* **2004**, *16*, 5650−5658.
(23) Gontard, N.; Ring, S. *J. Agric. Food Chem.* **1996**, *44*, 3474−3478.
(24) Urzendiwsky, I. R.; Pechak, D. G. *Food Struct.* **1992**, *11*, 301−314.
(25) McBierty, V.; Packer, K. *Nuclear Magnetic Resonance in Solid Polymers*; Cambridge University Press: Cambridge, U.K., 1993.
(26) Zhang, X.; Hoobin, P.; Burgar, I.; Do, M. D. *Biomacromolecules* **2006**, *7*, 3466−3473.
(27) Zhang, X.; Takegoshi, K.; Hikichi, K. *Macromolecules* **1992**, 25, 2336−2340.
(28) Zhang, X.; Do, M. D.; Dean, K.; Hoobin, P.; Burgar, I. *Biomacromolecules* **2007**, *8*, 345−353.
(29) Calucci, L.; Forte, C.; Galleschi, L.; Geppi, M.; Ghiringhelli, S. *Int. J. Biol. Macromol.* **2003**, *32*, 179−189.

BM0703719